The post-translational amino acid epimerase BotH defines a new group of atypical alpha/beta-hydrolase-fold enzymes

Asfandyar Sikandar[1,#], Laura Franz[1,#], Sebastian Adam[1], Javier Santos-Aberturas[2], Liliya Horbal[3], Andriy Luzhetskyy[3], Andrew W. Truman[2], Olga V. Kalinina[4,5], Jesko Koehnke[1,*]

[1]Workgroup Structural Biology of Biosynthetic Enzymes, Helmholtz Institute for Pharmaceutical Research Saarland (HIPS), Helmholtz Centre for Infection Research (HZI), Saarland University, Campus Geb. E8.1, 66123 Saarbrücken, Germany

[2]Department of Molecular Microbiology, John Innes Centre, Colney Lane, Norwich NR4 7UH, United Kingdom

[3]Department Microbial Natural Products, Actinobacteria Metabolic Engineering Group, Saarland University, Campus C2.3, 66123 Saarbrücken, Germany; HIPS, HZI, Germany

[4]Drug Bioinformatics Group, HIPS, HZI, Campus Geb. E8.1, 66123 Saarbrücken, Germany

[5]Medical Faculty, Saarland University, 66421 Homburg, Germany

[#]These authors contributed equally to this work

[*]To whom correspondence should be addressed: jesko.koehnke@helmholtz-hips.de

Abstract

D-amino acids endow peptides with diverse, desirable properties, but the post-translational and site-specific epimerization of L-amino acids into their D-counterparts is rare and very challenging. Bottromycins are ribosomally synthesized and post-translationally modified peptides that have overcome this challenge and feature a D-aspartate (D-Asp), which was previously proposed to arise spontaneously during biosynthesis. We have identified the highly unusual alpha/beta-hydrolase (ABH) fold enzyme BotH as a novel peptide epimerase responsible for the post-translational epimerization of L-Asp to D-Asp during bottromycin biosynthesis. To understand the mechanism of this reaction, we determined the structures of BotH and the BotH-substrate complex. We also found BotH to bind the natural product itself, which has implications for the regulation of bottromycin biosynthesis. Bioinformatic analyses of BotH homologs show that similar ABH enzymes are found in diverse biosynthetic gene clusters.

Introduction

Enzymes belonging to the superfamily of alpha/beta-hydrolase-fold proteins (ABHs) are found in all domains of life[1-3]. Their catalytic roles are highly diverse and they participate in primary and secondary metabolism, where they are usually responsible for the hydrolysis of (thio)ester and peptide bonds[4]. In addition, ABHs have also been reported to function as dehalogenases, epoxide hydrolases, dioxygenases, decarboxylases and haloperoxidases[3,4]. Despite low overall sequence conservation, ABH enzymes share a remarkably conserved core fold[2,3] that has a V-shaped lid domain above the active-site as a frequent addition[5,6]. A majority of ABH family members possesses a canonical Ser, His, Asp catalytic triad at the active-site, but other catalytic residues have also been observed[3,4]. In addition to catalytic roles, a ABH family members have also been reported to fulfil several other important functions, including small-molecule receptors that are involved in signal transduction, cell-cell interaction and channel regulation[5-8]. The ABH fold is thus a prime example for the reappropriation of a conserved core fold during evolution to fulfill a myriad of functions.

An aberrant ABH protein, BotH, is encoded in the biosynthetic gene cluster (BGC) for bottromycins[9-12]. This natural product family was first isolated from the terrestrial bacterium *Streptomyces bottropensis* and originally described as peptidic antibiotics with potent activity against Gram-positive bacteria[13,14]. Bottromycins are active against problematic human pathogens, such as Methicillin-resistant *Staphylococcus aureus*[15,16], address a novel target (the A-site of the prokaryotic ribosome)[17-19] and belong to the fast growing superfamily of ribosomally synthesized and post-translationally modified peptides (RiPPs)[9-12]. As is typical for RiPPs, their biosynthesis begins with the expression of a small structural gene to yield the precursor peptide (PP)[20]. Uniquely amongst bacterial RiPPs, the bottromycin PP contains an N-terminal core peptide (the eventual natural product) and a C-terminal follower peptide[9-12], which is important for substrate recognition by several of the biosynthetic enzymes[21,22]. The order of biosynthetic steps (and responsible enzymes) has since been proposed based on an untargeted metabolomics approach using mass spectral networking[23]. Subsequent *in vitro* work has largely corroborated the metabolomics data[21,22,24,25]. In the first phase of bottromycin biosynthesis, the N-terminal methionine is removed, proline, valine and phenylalanine residues of the core peptide are C-methylated and a cysteine-derived thiazoline is installed in no particular order[23]. The hallmark

macroamidine linkage is then formed in this intermediate[21,22], which is followed by proteolytic removal of the follower peptide to yield **1** (Figure 1A)[25].

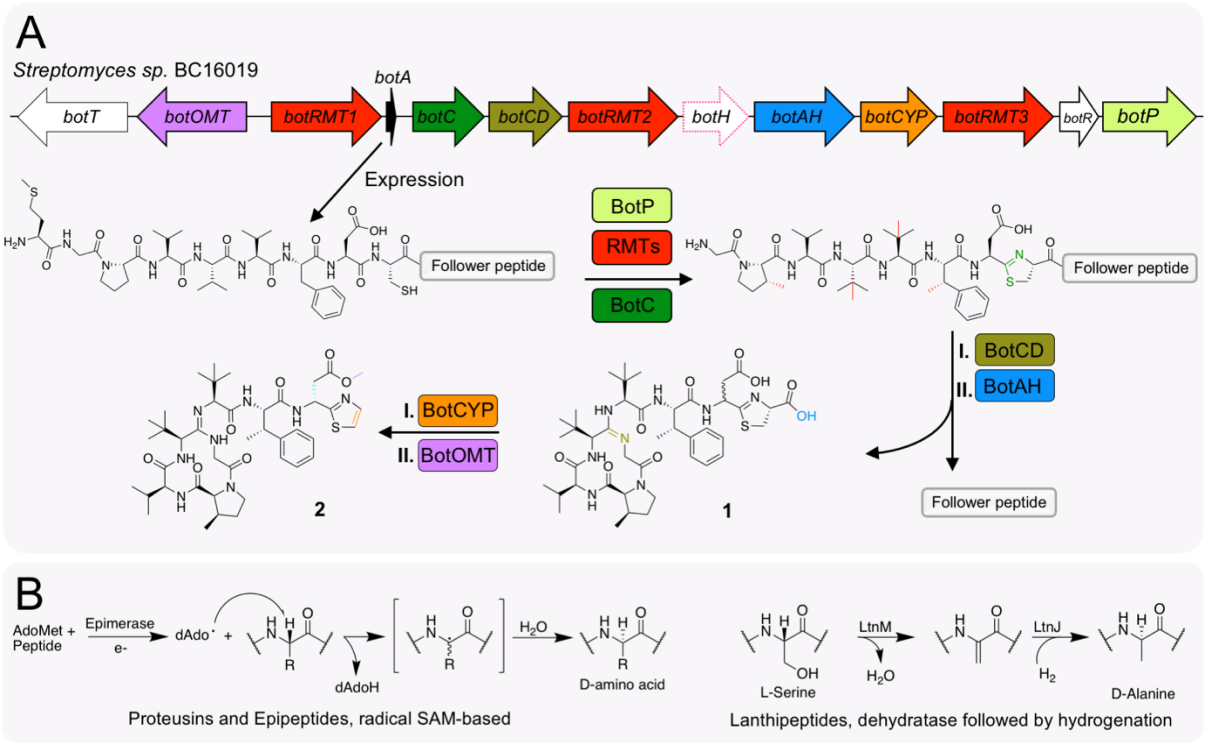

Figure 1: A Bottromycin BGC found in *S. sp.* BC16019. After expression of the precursor peptide BotA, its N-terminal methionine is removed by BotP, three radical methyl transferases (RMT) perform four C-methylations and BotC installs a cysteine-derive thiazoline. These initial steps appear to follow no particular order. Next, BotCD catalyzes formation of the macroamidine, after which BotAH removes the follower peptide to yield **1**. Oxidative decarboxylation (BotCYP) and O-methylation complete the biosynthesis of bottromycin A2 (**2**). Epimerization was proposed to occur spontaneously. Genes, enzymes and modifications have matching colors. White arrows represent genes for which no or a regulatory function have been proposed. The unusual ABH protein encoded in the pathway, BotH, is highlighted in pink. **B** Epimerization in RiPP biosynthesis reported to date. In proteusins, including polytheonamides, and epipeptides a radical SAM enzyme epimerizes a range of amino acids. In lanthipeptide biosynthesis, L-Ser can be converted to D-Ala in a two-step process.

To complete the biosynthesis of bottromycin A2 (**2**, Figure 1A), **1** undergoes epimerization, oxidative decarboxylation and O-methylation. While the latter two modifications have been attributed to specific enzymes, epimerization of the L-Asp of **1** was observed to progress spontaneously, albeit very slowly[23].

Amino acid epimerization in non-ribosomal peptide synthesis is usually catalyzed by epimerization domains embedded within the assembly line that function on carrier protein-bound aminoacyl substrates[26]. Due to their ribosomal origin, RiPPs must undergo post-translational epimerization after

the PP has been expressed as an all L-amino acid peptide. To date, only two enzymatic mechanisms for this process have been described in RiPPs, involving either a radical-SAM enzyme[27-30] or a two-step dehydration-hydrogenation process to generate D-alanine from L-serine[31,32].

Here, we report the identification of BotH, an unusual ABH enzyme from the bottromycin BGC, as the epimerase of the biosynthetic pathway. This is the first reported instance of an ABH enzyme catalyzing peptide epimerization and thus expands the catalytic scope of this vast enzyme family. Biochemical data together with the structure of the BotH–substrate complex allowed us to propose a mechanism for this reaction. Interestingly, BotH is also able to bind bottromycins with high affinity, which hints at additional function(s) in the biosynthetic process. We show that all canonical ABH active-site residues required for hydrolase activity are absent in BotH, and bioinformatic analyses indicate that BotH homologs with comparable non-hydrolytic residues are widespread amongst BGCs and may catalyze similar biosynthetic steps.

Results and Discussion

BotH is an unusual member of the ABH superfamily

In a search for an enzyme that may catalyze the epimerization in the bottromycin pathway, we noticed that the gene encoding for BotH had been annotated as an ABH, but that the predicted active-site residues (Ser/His/Asp) were not present and there were no prior experimental data on the role of this protein. We therefore expressed, purified and crystallized BotH (see Materials and Methods for details). A high-resolution (1.18 Å) native BotH dataset was collected from a crystal belonging to space group I222, which was phased using seleno-methionine BotH data (data collection and refinement statistics for all structures can be found in Table S1). The crystals contained one protomer in the asymmetric unit and the electron density for residues 10 – 262 was continuous in the refined model. BotH is comprised of the prototypical ABH core structure (Figure S1) and the putative active site was covered by a V-shaped loop consisting of four α-helices (Figure S1). A search for similar structures using the DALI server[33] revealed 3-oxoadipate-enol-lactonase (PDB 2xua)[34] as the closest structural homolog (Figure S1). A comparison of the two proteins revealed that in BotH, the active-site Ser has been mutated to a Phe, which is part of a Phe-Phe motif that spans a large, hydrophobic plane

at the active site (Figure S1). The remaining residues of the catalytic triad are either mutated (His to Ile) or missing (Asp) (Figure S1). In spite of these mutations, the sizeable cavity found in this region of the structure appeared to be large enough for binding **1**.

BotH catalyzes the epimerization of 3b and 3a

To confirm this hypothesis, a des-methyl analog of **1**, **3** (des-methyl Pro2, Val4, Val5 and Phe6), was enzymatically produced as reported previously (Figures 2A and S2)[25]. Careful analysis revealed **3** to exist as an epimeric mixture of **3a** (D-Asp) and **3b** (L-Asp) (Figures 2A and S3 – S5). When 20 μM **3a**/**b** was incubated with 5 μM BotH and the reactions were analyzed by high-resolution electrospray ionization liquid chromatography−mass spectrometry (HR-ESI-LCMS), we observed a change in **3a** : **3b** ratios (Figure 2B), which was BotH-concentration dependent within the 2 h time-scale of the experiment (Figure 2C): Increasing the BotH concentration resulted in a shift to **3a** (D-Asp), which is the required epimer to proceed with biosynthesis[35]. To probe if only **3b** or both epimers were substrates, we incubated **3a**/**b** with BotH in D_2O. This resulted in rapid (< 60 s) deuteron incorporation at the Asp7 position in both peaks, while very little deuteron incorporation was observed in the absence of BotH even after 24 hours (Figures 2D, S4 and S6). In fact, BotH concentrations low enough to leave epimer ratios unchanged still resulted in accelerated deuteron incorporation (Figure S6). Repeating this experiment using the deuterated sample in H_2O showed an equally rapid exchange with solvent protons back to **3a**/**b** (Figure S6). These data implied that BotH accepts both, **3a** and **3b**, as substrates in a reversible reaction, while favoring D-Asp (**3a**) as the product.

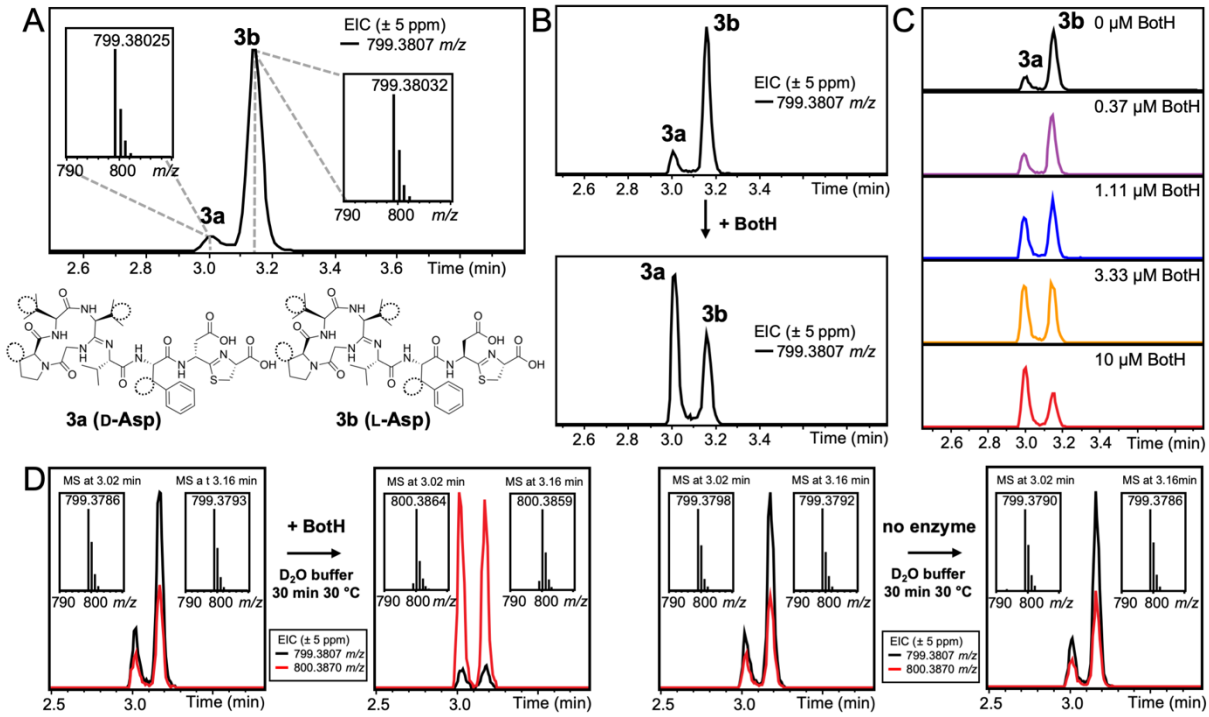

Figure 2: A Spontaneous epimerization of the Asp in position 7 after proteolytic removal of the follower peptide. Marfey's reagent was used to assign the stereochemistry of the Asp for both peaks (Figure S5). Extracted ion chromatograms (EIC) of **3** ($[M+H]^+_{calc.}$=799.3807; ± 5 ppm) and mass spectra at 3.00 and 3.15 min are shown. Missing methyl groups are highlighted by dashed ovals. **B** Incubation of **3a**/**b** with BotH results in a change of **3a** : **3b** ratios with **3a** (D-Asp) now the more abundant species. EICs of **3** ($[M+H]^+_{calc.}$=799.3807; ± 5 ppm) are shown. **C** Incubating 20 µM **3a**/**b** with increasing concentrations of BotH led to a shift of the equilibrium towards **3a**. Increasing BotH concentrations beyond 10 µM did not lead to a further shift of epimer ratios. EICs of **3** ($[M+H]^+_{calc.}$=799.3807; ± 5 ppm) are shown. **D** Deuteron incorporation into **3a/b** by BotH in D_2O buffer. EICs for **3** ($[M+H]^+_{calc.}$=799.3807; ± 5 ppm) (black) and deuterium incorporated **3** ($[M+H]^+_{calc.}$=800.3870; ± 5 ppm) (red), as well as mass spectra at the EIC maxima are shown. Representative experiments were repeated independently three times with similar results.

Structure of the BotH-3a complex

To better understand the mechanism of this intriguing enzyme, the high-resolution crystal structure of BotH in complex with its substrate **3a**/**b** was determined to 1.25 Å resolution. The overall structure of the complex was virtually unchanged when compared to the apo structure (C_α rmsd of 0.12 Å) (Figure S7). The substrate is curled into the active site in a way that places the thiazoline underneath the four amino acid macrocycle and the substrate engages in extensive hydrophobic interactions as well as inter- and intramolecular hydrogen bonds (Figures 3A and S7). Of particular note are hydrogen bonds of the thiazoline carboxy group with the backbone NH of Val41 and Phe110. These two BotH residues are in the position of the oxyanion hole found in many hydrolases. The carboxy group of the substrate's Asp7 is involved in a hydrogen bonding network with ordered water molecules that

ultimately link this side-chain to BotH residues (Figure S7). An intramolecular hydrogen bond links the substrate's carbonyl of Val3 with the backbone NH of Asp7. The best fit to the electron density is achieved by choosing the amidine resonance structure that places the double-bond inside the macrocycle and a D-Asp in position 7, which indicates that the ligand observed in the complex structure is **3a** (Figure S7). Since the epimerization mechanism would, at least formally, involve proton abstraction and addition, we scanned the complex structure for potential catalytic residues within 4 Å of the C_α hydrogen of Asp7, the site of catalysis, but could not identify any. This left two possibilities: bulk solvent or the side chain of substrate Asp7; its carboxy group is within 2.2 Å of the C_α hydrogen of interest. To probe the importance of the side chain identity in position seven for epimerization, we first tested the conservative mutant substrates Asp7Ala and Asp7Asn. While both substrates stabilized BotH in thermal shift assays comparable to **3a**/**b**, we observed no epimerization (Figure S8). The extension of the Asp7 side-chain by an additional methylene group (Asp7Glu), results in severely reduced turnover by BotH, but this substrate epimerizes (Figure S8). These data imply that a side-chain carboxy group in position 7 of the substrate is essential for catalysis and that the appropriate distance of this carboxy group relative to the residue's C_α proton has a significant impact on turnover, which suggests that the BotH reaction may be an example of substrate-assisted catalysis.

BotH has relaxed substrate specificity

We had previously reported that the enzymes used to generate **3a**/**b** possess relaxed substrate specificities for core-peptide residues 2 – 7 (Figure S9)[25]. Since substrate position 7 was restricted to Asp or Glu for epimerization, we wondered if BotH tolerates mutations in the remaining positions. To this end, a series of 13 BotA core-peptide mutants were used to produce the variant BotH substrates enzymatically. These substrates were then incubated with or without BotH and analyzed by LC-MS (Figures 3B and S10 - 11). All but two mutations in positions two to six were processed by BotH. The positions of Val5 and Phe6 are intimately connected and it appeared that the orientation of the Phe6 side-chain is critical for epimerization. In agreement with this hypothesis, Phe6Ala could not be epimerized by BotH while Phe6Tyr and Phe6Trp were substrates. The side-chain of position 5 (Val) is

engaged in hydrophobic interactions with the side-chains of Val4 and Phe6. Accordingly, Val5Thr is not a BotH substrate, while Val5Ala, Val5Leu and Val5Glu can be epimerized by the enzyme. The ability of BotH to process Val5Glu may appear surprising, but the flexibility of the Glu side chain should allow the C_β methylene of Glu5 to engage in hydrophobic interactions with Val4 and Phe6, while the C_γ methylene and terminal carboxy group point towards bulk solvent. Our data demonstrate that BotH is able to process a variety of substrates, which will be invaluable for the production of bottromycin derivatives.

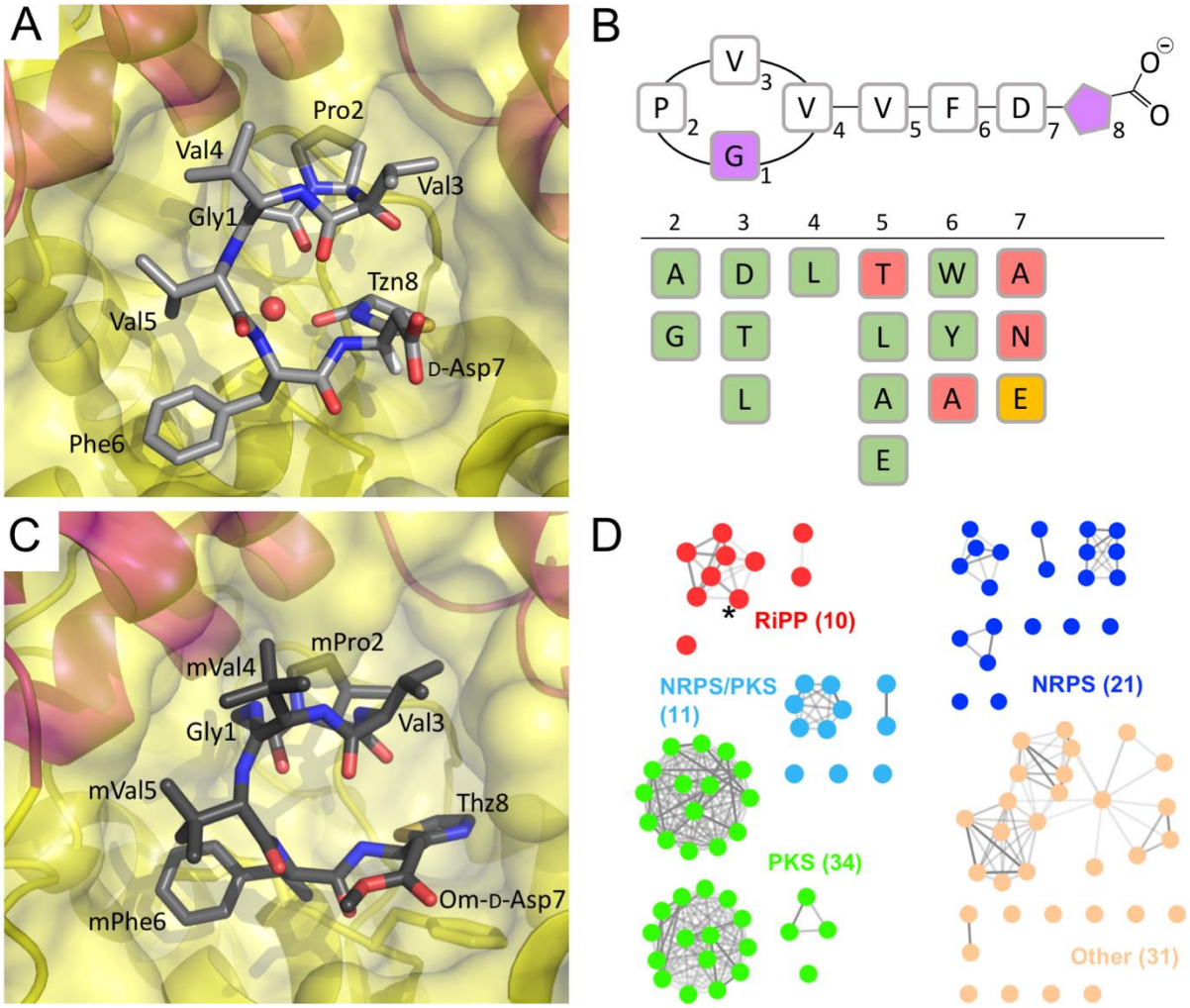

Figure 3: A Close-up of **3a** (gray sticks, labeled. Tzn = Thiazoline) bound in the BotH active site (cartoon, yellow/magenta with semi-transparent surface representation). The ordered water molecule trapped between substrate and protein is shown as a red sphere. The Asp7 C_α hydrogen is shown as a white stick for clarity. **B** Summary of BotA point mutants tested as BotH substrates. Purple positions cannot be varied (pentagon represents thiazoline). Accepted mutations are highlighted in green, orange indicates a poor substrate and red mutations cannot be processed by BotH. The accompanying HR-LCMS data can be found in Figures S10 – S11. **C** Same as **A**, but bottromycin A2 (dark gray sticks, labeled) bound to the active site of BotH. m = methylated residue, Om = O-methylated residue, Thz = Thiazole. **D** Sequence similarity network of ABHs homologous to BotH (marked with an asterix). Of

the 107 genes, 76 could be assigned to BGCs representing the three large bacterial natural product superfamilies (darker edges represent higher sequence similarity, NRPS = non-ribosomal peptide synthetase; PKS = polyketide synthase).

BotH binds bottromycins, which act as inhibitors of epimerization

Since **3a**/**b** are close structural homologs of bottromycin A2 (**2**), it seemed feasible that BotH may be able to bind to bottromycins. We thus performed microscale thermophoresis (MST) experiments using heterologously produced **2** and three closely related variants (**4** – **6**, Figure S12). BotH was able to bind all four bottromycins with K_D values in the high nM to low μM range but unable to epimerize oxidatively decarboxylated **3a** (Figure S12). To understand the mode of binding, we determined the crystal structures of three bottromycin–BotH complexes to 1.40 (**2**), 1.70 (**5**), and 1.48 (**6**) Å resolution, respectively (Figures 3C and S13 – 14). These also represent the first crystal structures of any bottromycin. As observed for the complex with **3a**, the overall structural change in BotH due to ligand binding was minimal (C_α RMSD < 0.2 Å) and the bottromycins bound in a similar manner as **3a** (Figures 3A and 3C). Despite the high resolution, it is not obvious which way the thiazole is flipped, since the loss of the carboxy group due to thiazoline oxidation allows a fit of both rotamers without inducing a clash with BotH (Figure S15). The bottromycins themselves are oriented in a twisted fashion that results in several tight, intramolecular hydrogen bonds (Figure S14). Compared to the published NMR structure[36], bottromycin A2 experiences significant strain as a result of binding to BotH, as it is forced to adopt a horseshoe shape with Val5 and Phe6 at its apex and the C-terminal thiazole stacked parallel under the macrocycle (Figure S16). As expected, bottromycin A2 acts as an orthosteric inhibitor of epimerization (Figure S17), which suggests that BotH may be involved in a biosynthetic feedback mechanism to prevent self-poisoning of the producing strain (Figure 4A).

In this model, an increase in the intracellular bottromycin concentrations offers a direct and faster means to reduce bottromycin production than altered gene expression since epimerization of Asp7 is highly important for the activity of the succeeding enzyme BotCYP[35]. It is of course also possible that BotH sequesters mature bottromycin to aid self-immunity.

The ability of BotH to bind both the substrate and the mature natural product with high affinity may serve as a cautionary tale for attempting to identify the binding partners of “non-catalytic” ABHs.

When using BotH to capture its ligand/substrate from either supernatant or lysate of a bottromycin producing strain, we were only able to detect bottromycin A2, but not the actual substrate **1** (Figure S18). Since biosynthetic pathway products tend to be present at higher concentrations than pathway intermediates, careful analysis of the biosynthetic pathway supplying the ligand is required to exclude additional, non-canonical catalytic function(s) of the ABH under investigation.

Evolution of BotH and its distribution amongst bacterial BGCs

ABHs comprise one of the largest protein families (~500,000 protein matches in InterPro[37], ~400,000 of them in Bacteria), of which 192,602 belong to Pfam[38] family PF00561 (Abhydrolase_1). The Ser-His-Asp catalytic triad is surprisingly poorly conserved: in 101,123 bacterial proteins from the PF00561 family, at least one of the catalytic residues is mutated or missing. In most cases (73,116 sequences), His is missing; and in the majority of these proteins (64,852 sequences) Asp is missing as well. Ser is mutated in only 42,810 sequences, most frequently to an aspartic acid, and completely missing in 1,283 sequences. Using these data, we identified 1,530 proteins that are unlikely to have hydrolase activity (see Materials and Methods section for details), including BotH. Taxonomic analysis revealed that these non-functional hydrolases are widespread among both Gram-positive and Gram-negative bacteria.

From these sequences, we then selected those that were in or near (less than 1 kb away) BGCs, which resulted in 107 proteins that were used to build a sequence–similarity network (Figures 3D and S19). In this network, all BotH homologs from bottromycin BGCs cluster together. Among the identified BGCs, two other major natural product superfamilies can be identified in addition to RiPPs: NRPS (non-ribosomal peptide synthetase) and PKS (polyketide synthase) clusters.

Conclusion

We have identified the enzyme BotH as the epimerase of the bottromycin BGC, which is selective for Asp and Glu, but promiscuous with regards to mutations at other positions of the substrate. Based on the biochemical and structural data, we propose the following mechanism for epimerization in bottromycin biosynthesis (Figure 4B): Cleavage of the follower peptide converts the 2-thiazoline

residue into a 2-thiazoline-4-carboxy moiety at the carboxy terminus of **3b**, which is bound by BotH. Interestingly, the two BotH residues that form hydrogen bonds with the thiazoline carboxy group are in the position of the canonical oxyanion hole found in most ABHs. By binding, **3b** traps an ordered water molecule within hydrogen-bonding distance of the thiazoline's nitrogen and carboxy group. The side-chain of Asp7 is positioned such that it may serve as a base to abstract the C_α proton from itself, which triggers enamine formation and leads to proton transfer from the ordered water molecule to the thiazoline nitrogen. The resulting hydroxide is still hydrogen bonded to the thiazoline's carboxy group and the thiazoline nitrogen proton. Abstraction of this proton by the hydroxide triggers reprotonation of the enamine by the side chain of Asp7 and results in epimerization. The inability of BotH to epimerize substrate with an Asp7Asn mutation suggests an essential role of the carboxylic acid side chain and thus substrate-assisted catalysis. As demonstrated by our hydrogen-deuterium-hydrogen exchange experiments, this reaction is fully reversible. We would like to note that the carboxy group of Asp7 is surrounded closely (O – O distances 2.5 – 3.1 Å) by four ordered water molecules (Figure S20), which appear well-positioned to facilitate the exchange of the abstracted proton/deuteron with bulk solvent during catalysis (Figure S20). It appears that lowering of the energetic barrier for epimerization by BotH is sufficient to supply the succeeding enzyme with sufficient substrate for complete turnover, even without changing the **3a** : **3b** ratios[35]. This situation is reminiscent of non-ribosomal peptide synthetases that can contain epimerase domains, which produce a mixture of D- and L-epimers of a particular amino acid. The succeeding enzyme (condensation domain) then provides the stereochemical resolution of the pathway through selective incorporation of the D-amino acid[39].

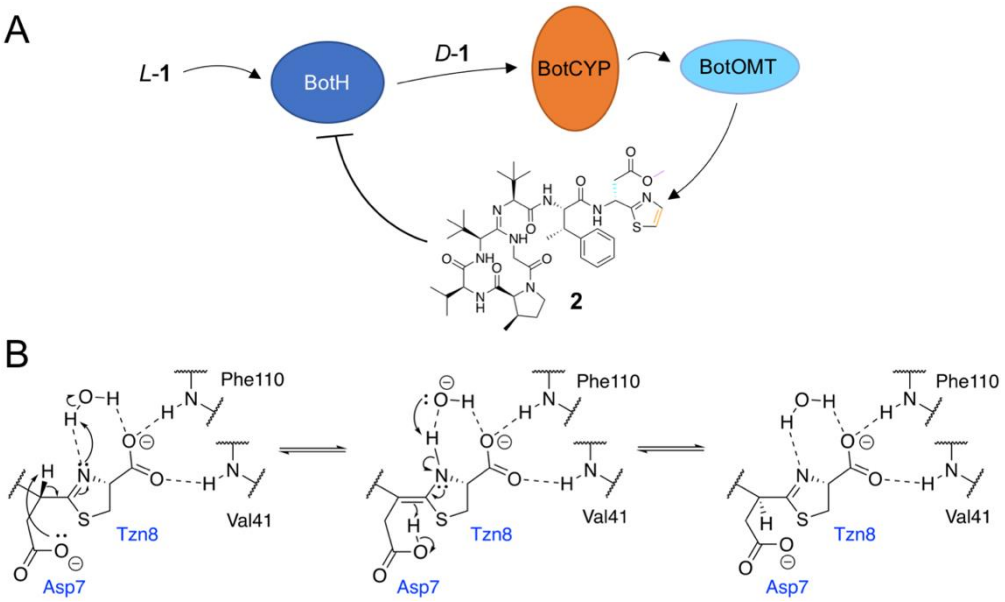

Figure 4: A Proposed role of BotH in bottromycin biosynthesis. A rise of intracellular bottromycin concentrations leads to an inhibition of BotH epimerase activity, which may in turn prevent self-poisoning of the producing strain and act as an intracellular buffer to store bottromycins. **B** Proposed mechanism for the epimerization of **3b** to yield **3a**. BotH residues are labeled in black, substrate residues in blue. Hydrogen bonds are shown as dashed lines. Ordered water molecules surrounding the Asp7 carboxy group are not shown for clarity (see Figure S20 for details).

It is still unclear why bottromycin A2 contains a D-Asp, as studies with synthetic derivatives have shown that both epimers display the same bioactivity[40]. Selectivity of the bottromycin exporter BotT appears possible, despite a very small fraction of bottromycin A2 in culture supernatant appearing to be the L-Asp epimer (Figure S21). The main benefit of epimerization may be providing increased resistance to proteolytic degradation of bottromycin, since D-amino acid containing peptides have longer half-lives[41,42]. It is of course also possible that the bottromycin target of organisms in a native setting requires a D-Asp for optimal target binding. Interestingly, the structure elucidation of novel bottromycin analogs via crystallization of their complex with BotH appears to require less compound and be more straightforward than NMR, due to the robust crystallization condition, high affinity and very well-diffracting crystals.

The presence of BotH-like ABH protein encoding genes in over 100 BGCs encoding for the biosynthesis of diverse secondary metabolites places BotH as the founding member of a new subfamily of non-classical ABH enzymes. It will be fascinating to explore the functions of selected homologs, which may be able to epimerize non-Asp stereocenters across families of secondary metabolites via the unprecedented mechanism we have identified for bottromycin.

Methods

Protein expression and purification

The BotH coding sequence was amplified from genomic DNA isolated from *Streptomyces* sp. BC16019 and cloned into the pET-28b plasmid (Novagen). The resulting construct was verified by enzymatic restriction digestion and DNA sequencing before being transformed into *E. coli* BL21(DE3) competent cells.

A single colony was selected and grown in LB liquid medium supplemented with kanamycin (50 μg / mL) to make an overnight culture. This culture was used at a dilution of 1 to 100 to inoculate fresh LB medium containing the appropriate antibiotic, and the culture was grown at 37 °C, 180 rpm. Upon reaching an optical density (OD_{600}) of 0.6, the cultures were transferred to a precooled shaker at 16 °C, and protein expression was induced by addition of 1 mM IPTG. The cells were grown at 16 °C and 180 rpm over night before being harvested by centrifugation. Cell pellets were stored at -80 °C until further use.

The cell pellets were resuspended in lysis buffer (20 mM Tris pH 8.0, 500 mM NaCl, 20 mM Imidazole, and 3 mM DTT) supplemented with 0.4 mg DNAse per gram of wet cell pellet and cOmplete EDTA-free protease inhibitor tablets (Roche). The cell suspension was lysed via passage through a cell disrupter (Constant Systems) at 30,000 psi, and cell debris was removed by centrifugation (40,000 x g, 4 °C, 15 min). The supernatant was collected and directly loaded onto to a 5 mL Histrap HP column (GE healthcare) preequilibrated with lysis buffer. The column was washed extensively with lysis buffer (30 CV) before the protein was eluted with lysis buffer supplemented with 250 mM imidazole. Fractions containing BotH were directly loaded onto a gel filtration column (HiLoad 16/600 Superdex 200 pg, GE healthcare) preequilibrated in gel filtration buffer A (20 mM HEPES pH 7.4, 200 mM NaCl, 1 mM TCEP). The fractions of the highest purity as judged by SDS-PAGE were pooled and concentrated to 5 mg / mL.

Crystallization and structure determination

For crystallization, BotH was treated with thermolysin (1 : 100) on ice for 2 h, after which the protein was passed over a HiLoad 16/600 Superdex 200 pg gel filtration column as described above and concentrated to 5 mg / mL. Crystals of apo BotH and BotH in complex with ligands were obtained at 18 °C in 1.2 - 1.8 M ammonium sulfate and 0.1 M Tris-HCl using the hanging drop vapor diffusion method. For the complex crystallization, the thermolysin-treated protein was incubated with excess ligand (1 - 2 mM) on ice overnight before setting up crystallization drops. Crystals appeared after a few days and were allowed to grow for an additional week. The crystals were cryoprotected in mother liquor supplemented with 30% glycerol and 0.5 mM ligand. Data was collected at ESRF (Beamlines ID23-1 and ID23-2), DESY (Beamline P11) and SLS (Beamline X06DA). To solve the apo structure, a single wavelength anomalous dispersion (SAD) data set was collected at the Se K absorption edge. Data were processed using Xia2[43], the structure was solved using PHENIX *AutoSol*[44] and the initial model used to obtain a molecular replacement solution for the high-resolution native data set using Phaser[45]. The solution was manually rebuilt in COOT[46] and refined using PHENIX Refine[44]. This apo structure was then used as a search model for structure determination of the complex crystal structures by molecular replacement (Phaser). Data for all complex crystal structures were processed using XDS[47] and POINTLESS[48], AIMLESS[49] and Ctruncate[50] implemented in ccp4[51]. All structures were validated using MolProbity. The images presented were created using PyMOL (Schrödinger, LLC) and LigPlot+[52].

Enzymatic reaction of BotH with **3**

To investigate the effect of BotH on **3a**/**b**, 20 µM **3a**/**b** were incubated with and without the addition of 5 µM BotH in GF buffer for 30 min. Reactions were stopped by the addition of 2 volumes ACN and were frozen at -80 °C until analysis. Reactions were set up and analyzed in at least triplicates.
To test the effect of different BotH concentrations on the **3a** : **3b** ratio, 20 µM **3a**/**b** were incubated with 0, 0.37, 1.11, 3.33 or 10 µM BotH at 30 °C for 2 h in GF buffer. Reactions were stopped by the addition of 2 volumes ACN and were frozen at -80 °C until analysis. Higher concentrations than

10 µM or longer incubation times were also tested, but did not lead to a further shift of epimer ratios. Reactions were set up and analyzed in triplicates.

To produce a roughly racemic mixture of **3a** : **3b**, 20 µM **3a**/**b** were incubated with 4 µM BotH for 30 min at 30 °C in GF buffer. BotH was denatured at 98 °C, 10 min, pelleted by centrifugation (15 min, 15,000 rpm) and the supernatant was lyophilized to remove all solvent.

Data availability

Atomic coordinates and structure factors have been deposited in the RCSB Protein Data Bank with accession codes 6T6H (BotH apo), 6T6X (BotH-**3a** complex), 6T6Y (BotH-**2** complex), 6T6Z (BotH-**5** complex), and 6T70 (BotH-**6** complex). Other relevant data supporting the findings of this study are available in this published article, its Supplementary Information files or from the corresponding author upon request.

Acknowledgements

We would like to thank the Swiss Light Source (X06DA), European Synchrotron Radiation Facility (ID23-1 and ID23-2) and Deutsches Elektronen Synchrotron (P11) as well as associated beamline staff for their support. We thank Prof. Shuichi Hirono and Prof. Hiroaki Gouda for providing the coordinate file of their solution NMR structure of bottromycin A2. J.K. is the recipient of an Emmy Noether Fellowship from the Deutsche Forschungsgemeinschaft (KO 4116/3-2). We thank Prof. Dr. Karsten Niefind and Dr. Rafael Guimaraes da Silva for critical reading of the manuscript and helpful suggestions.

Contributions

A.S. and J.K. established the production and purification of BotH. A.S. designed and performed crystallization experiments and determined the reported crystal structures. L.F. established BotH activity, carried out the biochemical experiments, produced BotH substrates and performed the mass

spectrometry. Marfey's analysis was carried out by L.F. A.S. and J.K. performed the MST experiments. A.S. produced and purified Bottromycin A2 and performed pull-down experiments. S.A. established the purification of the BotH substrate. J.S.-A. and A.W.T. aided bioinformatic analyses. L.H. produced, purified and analyzed Bottromycin A2 and derivatives under the guidance of A.L.. O.V.K. designed and performed the bioinformatic analyses and wrote the bioinformatics section. J.K. analyzed and visualized the crystal structures for publication and wrote the paper with contributions from all authors. The full program was carried out under the guidance and direction of J.K.

References

1 Ollis, D. L. *et al.* The alpha/beta hydrolase fold. *Protein Eng* **5**, 197-211, doi:10.1093/protein/5.3.197 (1992).

2 Nardini, M. & Dijkstra, B. W. Alpha/beta hydrolase fold enzymes: the family keeps growing. *Curr Opin Struct Biol* **9**, 732-737 (1999).

3 Mindrebo, J. T., Nartey, C. M., Seto, Y., Burkart, M. D. & Noel, J. P. Unveiling the functional diversity of the alpha/beta hydrolase superfamily in the plant kingdom. *Curr Opin Struct Biol* **41**, 233-246, doi:10.1016/j.sbi.2016.08.005 (2016).

4 Rauwerdink, A. & Kazlauskas, R. J. How the Same Core Catalytic Machinery Catalyzes 17 Different Reactions: the Serine-Histidine-Aspartate Catalytic Triad of alpha/beta-Hydrolase Fold Enzymes. *ACS Catal* **5**, 6153-6176, doi:10.1021/acscatal.5b01539 (2015).

5 Hamiaux, C. *et al.* DAD2 is an alpha/beta hydrolase likely to be involved in the perception of the plant branching hormone, strigolactone. *Curr Biol* **22**, 2032-2036, doi:10.1016/j.cub.2012.08.007 (2012).

6 Guo, Y., Zheng, Z., La Clair, J. J., Chory, J. & Noel, J. P. Smoke-derived karrikin perception by the alpha/beta-hydrolase KAI2 from Arabidopsis. *Proc Natl Acad Sci U S A* **110**, 8284-8289, doi:10.1073/pnas.1306265110 (2013).

7 Shimada, A. *et al.* Structural basis for gibberellin recognition by its receptor GID1. *Nature* **456**, 520-523, doi:10.1038/nature07546 (2008).

8 Marchot, P. & Chatonnet, A. Enzymatic activity and protein interactions in alpha/beta hydrolase fold proteins: moonlighting versus promiscuity. *Protein Pept Lett* **19**, 132-143, doi:10.2174/092986612799080284 (2012).

9 Crone, W. J. K., Leeper, F. J. & Truman, A. W. Identification and characterisation of the gene cluster for the anti-MRSA antibiotic bottromycin: expanding the biosynthetic diversity of ribosomal peptides. *Chemical Science* **3**, 3516-3521, doi:10.1039/C2SC21190D (2012).

10 Gomez-Escribano, J. P., Song, L., Bibb, M. J. & Challis, G. L. Posttranslational β-methylation and macrolactamidination in the biosynthesis of the bottromycin complex of ribosomal peptide antibiotics. *Chemical Science* **3**, 3522-3525, doi:10.1039/C2SC21183A (2012).

11 Hou, Y. *et al.* Structure and biosynthesis of the antibiotic bottromycin D. *Org Lett* **14**, 5050-5053, doi:10.1021/ol3022758 (2012).

12 Huo, L., Rachid, S., Stadler, M., Wenzel, S. C. & Muller, R. Synthetic biotechnology to study and engineer ribosomal bottromycin biosynthesis. *Chem Biol* **19**, 1278-1287, doi:10.1016/j.chembiol.2012.08.013 (2012).

13 Waisvisz, J. M. Bottromycin. I. A new sulfurcontaining antibiotic. *J. Am. Chem. Soc.* **79**, 4520-4521 (1957).
14 Nakamura, S. Isolation and characterization of bottromycins A and B. *J. Antibiotics, Ser. A* **18**, 47-52 (1965).
15 Sowa, S. *et al.* Susceptibility of methicillin-resistant Staphylococcus aureus clinical isolates to various antimicrobial agents. *Hiroshima J Med Sci* **40**, 137-144 (1991).
16 Shimamura, H. *et al.* Structure determination and total synthesis of bottromycin A2: a potent antibiotic against MRSA and VRE. *Angew Chem Int Ed Engl* **48**, 914-917, doi:10.1002/anie.200804138 (2009).
17 Otaka, T. & Kaji, A. Mode of action of bottromycin A2. Release of aminoacyl- or peptidyl-tRNA from ribosomes. *J Biol Chem* **251**, 2299-2306 (1976).
18 Otaka, T. & Kaji, A. Mode of action of bottromycin A2: effect on peptide bond formation. *FEBS Lett* **123**, 173-176 (1981).
19 Otaka, T. & Kaji, A. Mode of action of bottromycin A2: effect of bottromycin A2 on polysomes. *FEBS Lett* **153**, 53-59 (1983).
20 Arnison, P. G. *et al.* Ribosomally synthesized and post-translationally modified peptide natural products: overview and recommendations for a universal nomenclature. *Nat Prod Rep* **30**, 108-160, doi:10.1039/c2np20085f (2013).
21 Franz, L., Adam, S., Santos-Aberturas, J., Truman, A. W. & Koehnke, J. Macroamidine Formation in Bottromycins Is Catalyzed by a Divergent YcaO Enzyme. *J Am Chem Soc* **139**, 18158-18161, doi:10.1021/jacs.7b09898 (2017).
22 Schwalen, C. J. *et al.* In Vitro Biosynthetic Studies of Bottromycin Expand the Enzymatic Capabilities of the YcaO Superfamily. *J Am Chem Soc* **139**, 18154-18157, doi:10.1021/jacs.7b09899 (2017).
23 Crone, W. J. *et al.* Dissecting Bottromycin Biosynthesis Using Comparative Untargeted Metabolomics. *Angew Chem Int Ed Engl* **55**, 9639-9643, doi:10.1002/anie.201604304 (2016).
24 Mann, G. *et al.* Structure and Substrate Recognition of the Bottromycin Maturation Enzyme BotP. *Chembiochem* **17**, 2286-2292, doi:10.1002/cbic.201600406 (2016).
25 Sikandar, A., Franz, L., Melse, O., Antes, I. & Koehnke, J. Thiazoline-Specific Amidohydrolase PurAH Is the Gatekeeper of Bottromycin Biosynthesis. *J Am Chem Soc* **141**, 9748-9752, doi:10.1021/jacs.8b12231 (2019).
26 Hur, G. H., Vickery, C. R. & Burkart, M. D. Explorations of catalytic domains in non-ribosomal peptide synthetase enzymology. *Nat Prod Rep* **29**, 1074-1098, doi:10.1039/c2np20025b (2012).
27 Freeman, M. F. *et al.* Metagenome mining reveals polytheonamides as posttranslationally modified ribosomal peptides. *Science* **338**, 387-390, doi:10.1126/science.1226121 (2012).
28 Morinaka, B. I. *et al.* Radical S-adenosyl methionine epimerases: regioselective introduction of diverse D-amino acid patterns into peptide natural products. *Angew Chem Int Ed Engl* **53**, 8503-8507, doi:10.1002/anie.201400478 (2014).
29 Parent, A. *et al.* Mechanistic Investigations of PoyD, a Radical S-Adenosyl-l-methionine Enzyme Catalyzing Iterative and Directional Epimerizations in Polytheonamide A Biosynthesis. *J Am Chem Soc* **140**, 2469-2477, doi:10.1021/jacs.7b08402 (2018).
30 Benjdia, A., Guillot, A., Ruffie, P., Leprince, J. & Berteau, O. Post-translational modification of ribosomally synthesized peptides by a radical SAM epimerase in Bacillus subtilis. *Nat Chem* **9**, 698-707, doi:10.1038/nchem.2714 (2017).
31 Cotter, P. D. *et al.* Posttranslational conversion of L-serines to D-alanines is vital for optimal production and activity of the lantibiotic lacticin 3147. *Proc Natl Acad Sci U S A* **102**, 18584-18589, doi:10.1073/pnas.0509371102 (2005).

32 Yang, X. & van der Donk, W. A. Post-translational Introduction of D-Alanine into Ribosomally Synthesized Peptides by the Dehydroalanine Reductase NpnJ. *J Am Chem Soc* **137**, 12426-12429, doi:10.1021/jacs.5b05207 (2015).
33 Holm, L. Benchmarking Fold Detection by DaliLite v.5. *Bioinformatics*, doi:10.1093/bioinformatics/btz536 (2019).
34 Bains, J., Kaufman, L., Farnell, B. & Boulanger, M. J. A product analog bound form of 3-oxoadipate-enol-lactonase (PcaD) reveals a multifunctional role for the divergent cap domain. *J Mol Biol* **406**, 649-658, doi:10.1016/j.jmb.2011.01.007 (2011).
35 Adam, S., Franz, L., Milhim, M., Bernhardt, R. & Koehnke, J. Characterization of the stereoselective P450 enzyme BotCYP enables the in vitro biosynthesis of the Bottromycin core scaffold. (Submitted).
36 Gouda, H. *et al.* Three-dimensional solution structure of bottromycin A2: a potent antibiotic active against methicillin-resistant Staphylococcus aureus and vancomycin-resistant Enterococci. *Chem Pharm Bull (Tokyo)* **60**, 169-171, doi:10.1248/cpb.60.169 (2012).
37 Hunter, S. *et al.* InterPro: the integrative protein signature database. *Nucleic Acids Res* **37**, D211-215, doi:10.1093/nar/gkn785 (2009).
38 El-Gebali, S. *et al.* The Pfam protein families database in 2019. *Nucleic Acids Res* **47**, D427-D432, doi:10.1093/nar/gky995 (2019).
39 Stachelhaus, T. & Walsh, C. T. Mutational analysis of the epimerization domain in the initiation module PheATE of gramicidin S synthetase. *Biochemistry* **39**, 5775-5787, doi:10.1021/bi9929002 (2000).
40 Yamada, T. *et al.* Synthesis and Evaluation of Antibacterial Activity of Bottromycins. *J Org Chem* **83**, 7135-7149, doi:10.1021/acs.joc.8b00045 (2018).
41 Jungheim, L. N. *et al.* Potent human immunodeficiency virus type 1 protease inhibitors that utilize noncoded D-amino acids as P2/P3 ligands. *J Med Chem* **39**, 96-108, doi:10.1021/jm950576c (1996).
42 Rink, R. *et al.* To protect peptide pharmaceuticals against peptidases. *J Pharmacol Toxicol Methods* **61**, 210-218, doi:10.1016/j.vascn.2010.02.010 (2010).
43 Winter, G. xia2: an expert system for macromolecular crystallography data reduction. *Journal of Applied Crystallography* **43**, 186-190, doi:doi:10.1107/S0021889809045701 (2010).
44 Adams, P. D. *et al.* PHENIX: a comprehensive Python-based system for macromolecular structure solution. *Acta Crystallogr D Biol Crystallogr* **66**, 213-221, doi:10.1107/S0907444909052925 (2010).
45 McCoy, A. J. *et al.* Phaser crystallographic software. *J Appl Crystallogr* **40**, 658-674, doi:10.1107/S0021889807021206 (2007).
46 Emsley, P., Lohkamp, B., Scott, W. G. & Cowtan, K. Features and development of Coot. *Acta Crystallogr D Biol Crystallogr* **66**, 486-501, doi:10.1107/S0907444910007493 (2010).
47 Kabsch, W. Xds. *Acta Crystallogr D Biol Crystallogr* **66**, 125-132, doi:10.1107/S0907444909047337 (2010).
48 Evans, P. R. An introduction to data reduction: space-group determination, scaling and intensity statistics. *Acta Crystallogr D Biol Crystallogr* **67**, 282-292, doi:10.1107/S090744491003982X (2011).
49 Evans, P. R. & Murshudov, G. N. How good are my data and what is the resolution? *Acta Crystallogr D Biol Crystallogr* **69**, 1204-1214, doi:10.1107/S0907444913000061 (2013).
50 French, S. & Wilson, K. On the treatment of negative intensity observations. *Acta Crystallographica Section A* **34**, 517-525, doi:doi:10.1107/S0567739478001114 (1978).

51 Winn, M. D. *et al*. Overview of the CCP4 suite and current developments. *Acta Crystallogr D Biol Crystallogr* **67**, 235-242, doi:10.1107/S0907444910045749 (2011).
52 Laskowski, R. A. & Swindells, M. B. LigPlot+: multiple ligand-protein interaction diagrams for drug discovery. *J Chem Inf Model* **51**, 2778-2786, doi:10.1021/ci200227u (2011).